30

NASR-116
NsG-538

NASR-116
*
NsG-538

UNPUBLISHED PRELIMINARY DATA

Redistribution of Trapped Protons During a Magnetic Storm

by

Carl E. McIlwain

Department of Physics
University of California at San Deigo
La Jolla, California

April 1964

Abstract

15382 Abst

The first observation of a change in the distribution of high energy geomagnetically trapped protons which can be definitely attributed to the breakdown of adiabatic motion has been obtained with the aid of a scintillation detector aboard the Relay I satellite. Most of the observed variation in proton fluxes took place within a period of one day centered on 0 hours UT September 23, 1963, during the occurrence of the largest fluctuations in the earth's magnetic field in almost two years. The intensity of protons with energies greater than 34 Mev decreased by over a factor of ten in the region $L > 2.50$ earth radii and $B > .05$ gauss but changed by less than 10% in the region $1.80 > L > 2.10$. The character of the changes were such that previous events of this type could have produced the anomalous characteristics of the initial distribution.

Author

I. Introduction

It has been shown (Lenchek and Singer 1962) that within L = 1.5 earth radii the observed intensity and distribution of geomagnetically trapped protons with energies greater than 50 Mev can be accounted for (at least within a factor of 10) by cosmic ray produced neutron injection and atmospheric losses. The relative absence of high energy protons on high lines of force has led to the conclusion that there must be a breakdown of the conditions necessary for adiabatic motion which reduces the residence time of protons to much less than that predicted by atmospheric losses alone.

The theoretical work on non-adiabatic motion can be divided into two categories: 1. that concerned with effects of large larmor radii compared to the magnetic field gradients and 2. that concerned with the effects of fluctuations in the geomagnetic field. Observations presented here and elsewhere (McIlwain 1963, Fillius and McIlwain 1964) indicate that effects due to magnetic fluctuations are far more important that the effects which would occur in a static field.

While the observed spatial dependences appear to require that the motion of the energetic protons be perturbed by magnetic fluctuations, the data presented here represents the first definitive observation of an actual occurrence of this phenomenon. Time changes in trapped proton intensities have been observed previously (Pizzella, McIlwain, and Van Allen 1962, McIlwain 1963) but it cannot be shown that they were caused by magnetic fluctuations or in the case of geiger tube measurements, that they were not due to electron contamination.

II. Description of Experiment

This paper is primarily concerned with the results obtained by an omnidirectional scintillation counter aboard the Relay I satellite. Relay I was launched December 13, 1962, into an orbit with an apogee of 2.07 earth radii, a perigee of 1.21 earth radii and an inclination of 47.5 degrees. The precession of the orbit is such that the complete spatial distribution of trapped particles in the region $1.15 > R > 2.2$ earth radii and $\lambda < 60$ degrees (magnetic coordinates) can be obtained within a period of 140 days.

The detector consists of a 0.93 cm diameter sphere of plastic scintillator which is shielded by a uniform 1.30 g/cm^2 of aluminum over a full 2π steradians. The detector protrudes from the satellite structure to keep the front 2 π solid angle unobstructed. The back 2π solid angle is shielded by a minimum of 3.5 g/cm^2. A single channel integral discriminator was initially set to respond to pulses corresponding to energy losses in the scintillator of greater than 1.1 Mev. During the first one or two months in orbit, the effective discrimination level increased to about 1.7 Mev (presumably due to radiation damage). This change reduced the relative efficiency for counting penetrating electrons from about 10% to about 1%. The pulse height distribution produced by penetrating electrons decreases rapidly above 1.7 Mev such that a 1% change in discrimination level would cause the counting rate due to electrons to change by about 10%. The constancy of the electron produced counting rates in the region around L = 1.4 (where very high intensities of artifically injected electrons continue to reside) indicates that since May 1, 1963, the effective discrimination level has changed less than 10%. The characteristics listed below correspond to the final discrimination level of 1.7 Mev.

The relative efficiency for protons was experimentally measured to rise from less than 5% at 32.5 Mev to over 90% at 34 Mev and agrees well with the calculated threshold of 33.5 Mev. The calculated efficiency times geometric factor = ϵG remains a constant 0.33 cm^2 between 34 and 55 Mev and slowly rises to about 0.5 cm^2 at 100 Mev. Between 100 and 300 Mev, the calculated ϵG remains between .4 and .6 cm^2. In the region of space which will be discussed in this paper, the proton energy spectrum decreases with increasing energy with sufficient rapidity that less than 10% error is made in assuming ϵG is a constant 1/3 cm^2 above 34 Mev.

The efficiency for electrons has not been directly measured but various experiments and calculations indicate that assuming an ϵG of .003 cm^2 above 3.5 Mev and zero at lower energies would typically result in errors of less than a factor of two.

The pulses from the preamplifier are clipped by a delay line to a length of 0.25 microsecond. The first binary scaler has a stable deadtime of 3.3 microseconds. This is sufficiently short that the deadtime corrections in the data reported here are typically less than one percent.

III. Method of Data Reduction

The pulses from the detector are first sent through two binary scalers and are then sent to a 27 bit register which accummulates continuously without resetting. The contents of the 27 bit register are telemetered once each second. In practice, the counting rate varies slowly so that it is possible to take 12 second averages.

The measured cosmic ray counting rate of 0.6 counts per second is subtracted to yield the true intensity of trapped particles. In most cases this represents a relatively small correction.

The usual B, L magnetic coordinate system (McIlwain 1961) is used to organize the data. The Jensen and Cain (1962) representation of the earth's magnetic field was used in the computation of B and L. For many purposes, it is found convenient to interpolate the 12 second averages to a particular set of L values such as 1.80, 1.85, 1.90, etc.

After interpolation, the data are sorted with respect to B for each L value. After ordering in this fashion it is easy to detect any errors that may be present due to faulty data transmission. In practice, less than one error per 1000 data points was detected. Before deletion, the original records were examined to be certain that each faulty datum was actually due to noisy data transmission. Since the errors of this type tend to be large compared to the normal scatter in the data, it is regarded as unlikely that many if any, errors remain undetected.

IV. The Magnetic Storm

During the period 2000 UT September 22 to 0600 UT September 23 of 1963, the largest fluctuations in the earth's magnetic field since October 1961, occurred. The character of these fluctuations as observed below the ionosphere can be seen in Figure 1. The Fredricksburg magnetic observatory is at an L value of about 2.7 earth radii, therefore, the low frequency fluctuations observed at this station may be directly related to the fluctuations occurring in the region of space in which the motions of trapped protons were perturbed.

The large fluctuations seen in Figure 1 comprise only a part of the disturbed period which begain with a sudden commencement at 1414 UT September 21 and persisted up to 2300 UT September 23.

An examination of the rapid run magnetograph made at Fredricksburg reveals that there were important components in the power spectrum of the fluctuations over the entire observable range (about 0.1 to .0001 cycles/sec). The actual power spectrum has not been obtained due to the difficulty in converting the analog traces into digital readings suitable for analysis on a computer. The rapid run magnetograph made at College, Alaska, reveals the occurrence of giant micropulsations with amplitudes up to ± 40 gammas and a frequency of around 0.01 cycles/sec.

V. Pre-Storm Distribution

The intensities observed on lines of force with L values between 1.75 and 2.85 earth radii during the period May 1 to September 22, 1963, are shown as functions of B in Figure 2. Measurements of the electron fluxes in this region of space by other detectors aboard the Relay I satellite indicate that the flux of electrons with energies greater than 3.5 Mev was no more than three times the flux of protons with energies greater than 34 Mev. The data in Figure 2 is therefore probably contaminated by less than 3% by the electrons which were artificially injected in this region in 1962. This conclusion is supported by the extreme stability of the counting rates during this time period compared with the relatively rapid decreases in high energy electron fluxes observed earlier (McIlwain, 1963) in this region of space. The absolute intensities of protons obtained by this detector agree well with the proton intensities obtained by a solid state telescope also aboard the Relay I satellite.

The curves in Figure 2 correspond to weighted least squares fits to the data using the functional form $\mathrm{Ln}\, J_o = A_1 + A_2 T(\text{days}) + \sum_{n=1}^{5} A_{n+3}(B/B_o)^n$. The time coefficient A_2 was used to normalize to data to day 200 of 1963. During this period, the time coefficients A_2 were uniformly less than 8×10^{-4}/day so that the normalization in time required changes of less than 7%. Data points are shown for every fourth line to illustrate the distribution and scatter of the data. The curves in Figure 2 deviate from the data by as much as 5%, therefore an improved set of analytic fits was subsequently made by extending the power series up to n = 6. These new fits appear to have a relative accuracy of better than ± 3% in the regions where the intensity is greater than 300 protons $\text{sec}^{-1}\ \text{cm}^{-2}$. The average scatter of the data points is generally less than ± 4%.

It should be pointed out that the L dependence of the intensities is such that a one percent error in L would produce an error in the intensity of 10 to 30%. The use of a less accurate parameter such as $L_o = (M/B_{min})^{1/3}$ as suggested by Stone (1963) would therefore be expected to introduce an appreciable amount of additional scatter in the present data.

The omnidirectional intensities shown in Figure 2 have been used to derive the unidirectional intensities perpendicular to the magnetic field by the method outlined by Ray (1960) and Farley and Sanders (1962). The results of these computations are shown in Figure 3. The solution for the unidirectional intensity depends to first order upon the first derivative of the omnidirectional intensity with respect to B thereby amplifying any errors present in the omnidirectional measurements and analytic fits. Since it is extremely difficult to obtain the probable error in the derivative of an analytic fit, it is not possible to derive true probable errors for the curves in Figure 3. It is felt however, that the errors are typically less than 5%.

The rapid decrease in intensity toward high L values which demands the occurrence non-adiabatic processes is obvious in Figures 2 and 3. Another feature of the spatial distribution which demands the occurrence of non-adiabatic processes is the rapid increase in the intensities with decreasing B below 0.1 gauss. In the region of $B > 0.15$ gauss the unidirectional intensity perpendicular to the magnetic field varies approximately as the reciprocal of the average air density ($1/\bar{\rho}$) as predicted by theory (Ray 1960). At B values of less than .06 gauss, $1/\bar{\rho}$ increases by less than 60% with decreasing B so that the observed increases in intensity of up to a factor of ten cannot be due to a variation in the atmospheric loss rate.

VI. Post-Storm Distribution

The distribution shown in Figure 2 changed almost discontinuously within a period of hours at the time of the magnetic storm described earlier. Almost all of the change had taken place by September 24, 1963, after which the new distribution has been maintained for at least five months to a degree of constancy comparable to that of earlier distribution.

The data for the period September 24, 1963, to February 28, 1964, has been analyzed in the same manner as the data for the earlier period. The results are shown in Figures 4 and 5. The distribution on lines of force greater than L = 2.5

cannot be reliably obtained from the present data due to the very low intensities of protons in this region and the fact that a "new" outer zone of energetic electrons began to form after the magnetic storm which had its peak intensity at L values as low as 2.8. Extrapolations of the electron distribution indicates that there is an electron contamination in the data shown for L = 2.45 and 2.50 of up to 20% but that at L values of 2.40 and less the contamination is probably less than 5% at all times.

A comparison of Figures 3 and 5 reveals that the character of the changes produced by this storm is the same as that which would be required of previous events to have yielded the distribution shown in Figure 3. Explicitly, the anomalous character of Figure 3 has been made even more pronounced: the decrease with respectto L was made even more rapid and the relative increase toward low B values was made even larger.

The curves in Figures 3 and 5 have been used to obtain the contours of constant intensity in B L space as shown in Figure 6. In this figure, it can be seen that there was little change at L values of less than 2.1 but that in the region L > 2.4 the intensities were drastically reduced.

Three attempts to reveal the character of the change more explicitly are seen in Figures 7, 8, and 9. In Figure 7, it can be seen that the L dependence of the change depends strongly upon the B value. This is shown more clearly in Figure 8 in which the ratio of the unidirectional intensities is plotted versus B/B_o where $B_o = M/L^3$. An extrapolation of these curves up to the magnetic equator ($B/B_o = 1.0$) reveals that there may have been little change on <u>any</u> line of force at the equator. It is indeed quite possible that the equatorial intensities on high lines of force may have even increased. It is clearly of some importance that a properly instrumented satellite be put into an orbit which traverses this higher region of space before another large magnetic storm occurs. In Figure 9, the differences in absolute intensities are plotted versus L for two values of B/B_o. In this figure, it can be seen that the actual change in the intensities was relatively small, that is, where the relative change was large, the pre-storm intensities were low. The bars in this figure do <u>not</u> represent the probable errors but instead represent $\pm$ 2% of the pre-storm intensities. The curves in Figures 8 and 9 were computed directly from the improved fits mentioned earlier so that it is possible that the probable errors are as small as the

bars in Figure 9. In any case, the consistency of the independent computations at the different L values indicates that the probable errors are not as large as ± 5%. The reality of numerous small anomalies such as the strange L dependence of the ratios at $B/B_o = 1.3$ cannot be proven until a more thorough error analysis has been made.

VII. Detailed Time Dependence

In Figure 10, the time dependence of the omnidirectional intensity at L = 2.35 is shown for two ranges of B. The B dependences shown in Figures 2 and 4 have been used to normalize the data before and after the storm to B values of 0.045 and 0.12 gauss. The stability of the intensities before and after the event can be clearly seen. Figures 11 and 12 show the time dependence of the intensities on other lines of force and have been normalized to B = .045 and 0.12 gauss respectively.

The time coefficients (A_2) obtained from fitting the entire set of data obtained after September 27, 1963, for each line of force is generally uniformly positive but was less than 8×10^{-4}/day for all lines of force between L = 1.75 and 2.40. In Figure 12, it can be seen that the time coefficient is somewhat larger in the range B = .14 to .18 (the + symbols). Even in this region the time coefficients are generally less than 3×10^{-3}/day corresponding to a time constant (for changing by a factor of e = 2.72) of about one year. The apparent rate of increase is about .1 to .3 protons sec^{-1} cm^{-2} per day and is of the same order of magnitude predicted for neutron injection.

It is important to note that on five occasions during the present observations, magnetic storms occurred with low frequency magnetic fluctuations approximately one third the size of those measured during the September 23 storm. In Figures 10, 11, and 12, at the times of these events: days 157, 232, 257, 297, and 302 of 1963, it can be seen that these storms caused no permanent change as large as 10% and probably no instantaneous effects larger than 30%. It would appear that either the low frequency fluctuations are not a good indicator of the magnitude of the fluctuations in the frequency range which perturb the motion of protons or that there is a threshold effect. In this regard, it seems possible that some criteria for plasma instabilities may have been satisfied during the September 23 storm but not during the other events. In any case, it is important that all available magnetic records be searched for effects which are peculiar to the September 23 storm.

It is of considerable interest to determine the behavior of the protons during the storm. Fortunately, data was taken during two brief periods on each of the days September 22 and September 23, 1963. This data plotted versus L can be seen in Figures 13 and 14. Also shown in these figures are the intensities which would have been encountered by the satellite before and after the storm as given by Figures 2 and 4. Note that the vertical scale changes from logarithmic to linear below 10 protons sec^{-1} cm^{-2}. Some data points are negative due to statistical scatter and the subtraction of the cosmic ray contribution to the counting rate. On the left side of Figure 13, it can be seen that the intensities at $L < 2.64$ were unperturbed early on September 22. On the left side of Figure 14, it can be seen that by 1940 UT on September 22, small decreases had already occurred at L values as low as 2.5. Referring to Figure 1, it can be seen that this time is before the onset of the large low frequency fluctuations but is after the onset of the small higher frequency fluctuations. On the right side of Figure 13, it can be seen that by 0212 UT on September 23, the intensity at $L = 2.57$ was less than 2 protons sec^{-1} cm^{-2} compared with at least 30 protons sec^{-1} cm^{-2} only 6.5hrs. earlier (as given by the data taken at 1940 UT September 22 corrected for the difference in B) and with the pre-storm value of 60 protons sec^{-1} cm^{-2}.

The data on the right side of Figure 14 shows that by 1704 UT on September 23, a large fraction of the total change had already occurred at all L values. The intensities in the region $L = 2.35$ to 2.45 and $B = .04$ to .05 did not reach their final values until about three days later. While the intensities in this region were 20 to 50% high for these three days, the effect could be produced by an error in L of only 1%. It seems quite possible that large numbers of low energy particles were accelerated or injected at the time of the storm (a "ring current"?) thus perturbing the DC magnetic field in this region in such a manner that the motion of the lines of force and the adiabatic betatron acceleration of the high energy protons produced the observed effects.

VIII. Discussion

A complete understanding of this event is not possible before another dimension, the dependence upon energy, has been added to the experimental picture. A preliminary examination of the data received from the other proton detectors

aboard the Relay I satellite indicates that the relative changes in the fluxes of protons with energies between 18.2 and 35 Mev were rather similar to the changes reported here but that the fluxes of protons with energies greater than 5.2 Mev underwent no first order changes. Data from the Relay II satellite, which was launched January 21, 1964, indicates that the fluxes of protons with energy greater than 1.1 Mev are slightly higher than they were one year earlier.

Considering the size and frequency spectrum of the magnetic fluctuations, it appears certain that at least the third (or flux) adiabatic invariant of the high energy proton motion was violated. Some features of the observed intensity changes are more easily predicted by assuming that the second (or integral) and the first (or magnetic moment) invariants were also violated. While violations of these kinds probably also occurred, it is still of interest to consider the violation of the third invariant explicitly since this is required to achieve a substantial diffusion in the radial direction.

If the first two invariants μ and J are assumed to be constant, then in the non-relativistic limit we have

$\mu = p^2/2mB = E/B = \text{const}$ where B is the scalar magnitude of the magnetic field at the mirror point, m is the mass, and p is the momentum of the particle

and $J = \int_A^{A'} p_{||}\, ds = Ip = I\sqrt{2mE} = \text{const}$

Now L is defined (McIlwain 1961) by the equation

$$L^3\, B/M = F(I^3\, B/M)$$

so that if the violation of the third invariant changes the particle energy from E to E_1 (and B to $B_1 = B\, E_1/E$) then I changes to $I_1 = I\sqrt{E/E_1}$ and the new L value is given by

$$L_1^3\, B_1/M = F(I_1^3 B_1/M) = F[I^3(E/E_1)^{3/2}\, B_1/M]$$

Figure 15 shows the motion of the mirror point in B L space given by this equation as the particle energy varies over a wide range. The values of I = J/p

(in earth radii) at L = 2.0 are used to label the different cases. Also shown are four traces of constant magnetic latitude (i.e. radial lines in polar coordinates) and the trace for a constant radial distance of R = 1.10 earth radii. When particle motion reaches this trace they are rapidly removed by atmospheric loss. It can be seen that the possible motion of a particle's mirror point under the constraint that the first two invariants are constant is essentially radial with a slight tendency to move toward the magnetic equator.

One of the oldest ideas for explaining the presence of trapped protons is that solar protons are perturbed into trapped orbits in the outer limits of the geomagnetic field and are subsequently diffused inward. This concept has been considered independently by many people, but as yet, it has not been shown explicitly that the fluctuations in the distant field are adequate to perturb significant numbers of solar protons into trapped orbits or that the field fluctuations within the magnetosphere are adequate to diffuse a reasonable fraction of these down to low L values. It is to be hoped that a thorough analysis of the September 23 storm and its effects on the trapped protons will give some indication of the magnitude of the radial diffusion which can occur.

IX. Summary

The flux of geomagnetically trapped protons with energies greater than 34 Mev were observed to change almost discontinuously from one apparently stable distribution to another stable distribution during a magnetic storm. Some of the more important observations were that:

1. The change was in perfect time coincidence with large fluctuations in the magnetic field.
2. Most of the change occurred in less than 24 hours.
3. Large changes took place in only 6.5 hours.
4. Five smaller storms produced no observable effects.
5. The relative change increased rapidly toward higher L values.
6. The relative change increased with increasing B.

Aknowledgements

The author wishes to thank A. Dave' and A. Hassitt for their aid in the reduction and analysis of the data and the personnel at the Goddard Space Flight Center for their contributions to the success of this experiment. This research was supported in part by NASA contracts NAS5-1683, NASr-116, and NSG-538.

References

J.A. Farley and N.L. Sanders, "Pitch angle distributions and mirror point densities in the outer radiation zone", J. Geophys. Res., 67, 2159-2168, 1962.

Fillius, R.W. and McIlwain, C.E., "The anomalous energy spectrum of protons in the earth's radiation belt", submitted to Physical Review Letters, April 1964.

D.C. Jensen and J.C. Cain, "An interim geomagnetic field", J. Geophys. Res., 67, 3568(a), 1962.

Lenchek, A.M. and S.F. Singer, "Geomagnetically trapped protons from cosmic ray albedo neutrons", J. Geophys. Res., 67, 1263-1287, 1962.

McIlwain, C.E., "Coordinates for mapping the distribution of magnetically trapped particles," J. Geophys. Res., 66, 3681-3691, 1961.

McIlwain, C.E. and G. Pizzella, "On the energy spectrum of protons trapped in the earth's inner Van Allen zone", J. Geophys. Res., 68, 1811-1823, 1963.

McIlwain, C.E., "The radiation belts, natural and artificial", Science, 142, 355-361, 1963.

E.C. Ray, "On the theory of protons trapped in the earth's magnetic field", J. Geophys. Res. 65, 1125-1134, 1960.

E.C. Stone, "The physical significance and application of L, B_o, and R_o to geomagnetically trapped particles," J. Geophys. Res., 68, 4157-4166, 1963.

Figure Captions

Figure 1 Magnetograph made at Fredricksburg, Va., during the September 22 - 23 1963 storm.

Figure 2 The omnidirectional intensities of protons with energies greater than 34 Mev as a function of B along lines of force between L = 1.75 and 2.85 during the 144 day period prior to the storm.

Figure 3 The unidirectional intensities perpendicular to the magnetic field derived from the data shown in Figure 2.

Figure 4 Same as Figure 2 except for the 154 day period after the storm.

Figure 5 The unidirectional intensities perpendicular to the magnetic field derived from the data shown in Figure 4.

Figure 6 Contours of constant unidirectional intensities before and after the storm. Four contours per decade are given, corresponding to a factor of $10^{0.25} = 1.78$ in intensity between adjacent contours.

Figure 7 Ratios of the omnidirectional intensities versus L for three values of B.

Figure 8 Ratios of the unidirectional intensities versus B/B_o for seven values of L.

Figure 9 Changes in the absolute unidirectional intensities versus L for B/B_o equal 1.5 and 3.0. The bars correspond to ± 2% of the initial intensities, not the probable errors.

Figure 10 The time dependence in the omnidirectional intensities at L = 2.35 for two ranges of B.

Figure 11 The time dependence in the omnidirectional intensities on six lines of force at B values between .03 and .06 gauss.

Figure 12 The time dependence in the omnidirectional intensities on seven lines of force at B values between .06 and .18 gauss.

Figure 13 Intensities measured along the satellite trajectory just before and during the magnetic storm. Also shown are the intensities that would have been found along these trajectories before and after the storm. Note the change to a linear scale below the intensity of 10 protons sec^{-1} cm^{-2}.

Figure 14 The same as Figure 13 except at somewhat lower B values during the storm.

Figure 15 The solid lines correspond to the possible motion of the mirror point of a trapped particle in B L space under the constraints that the first and second invariants remain constant.

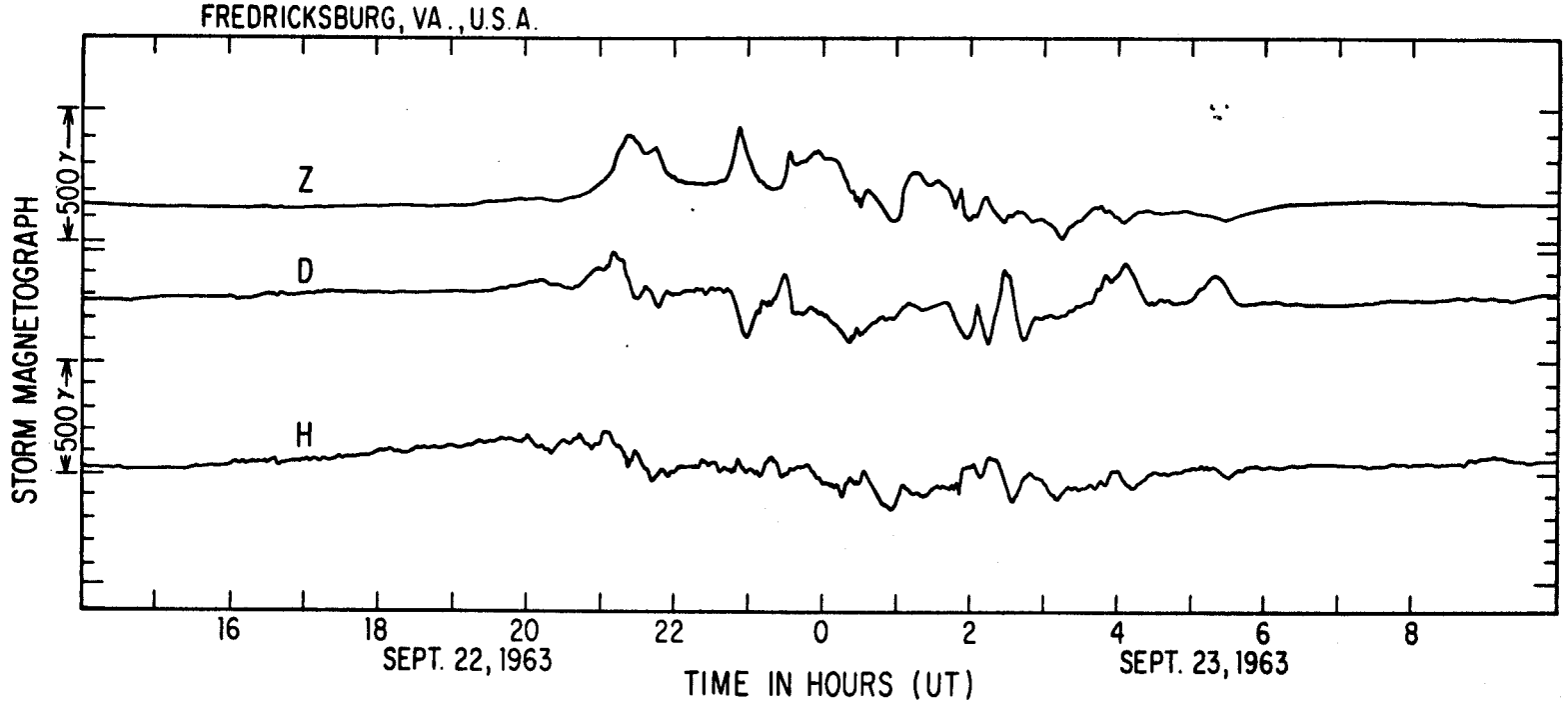
FREDRICKSBURG, VA., U.S.A.
STORM MAGNETOGRAPH
500γ
Z
D
500γ
H
16
18
20
22
0
2
4
6
8
SEPT. 22, 1963
SEPT. 23, 1963
TIME IN HOURS (UT)

Figure 1

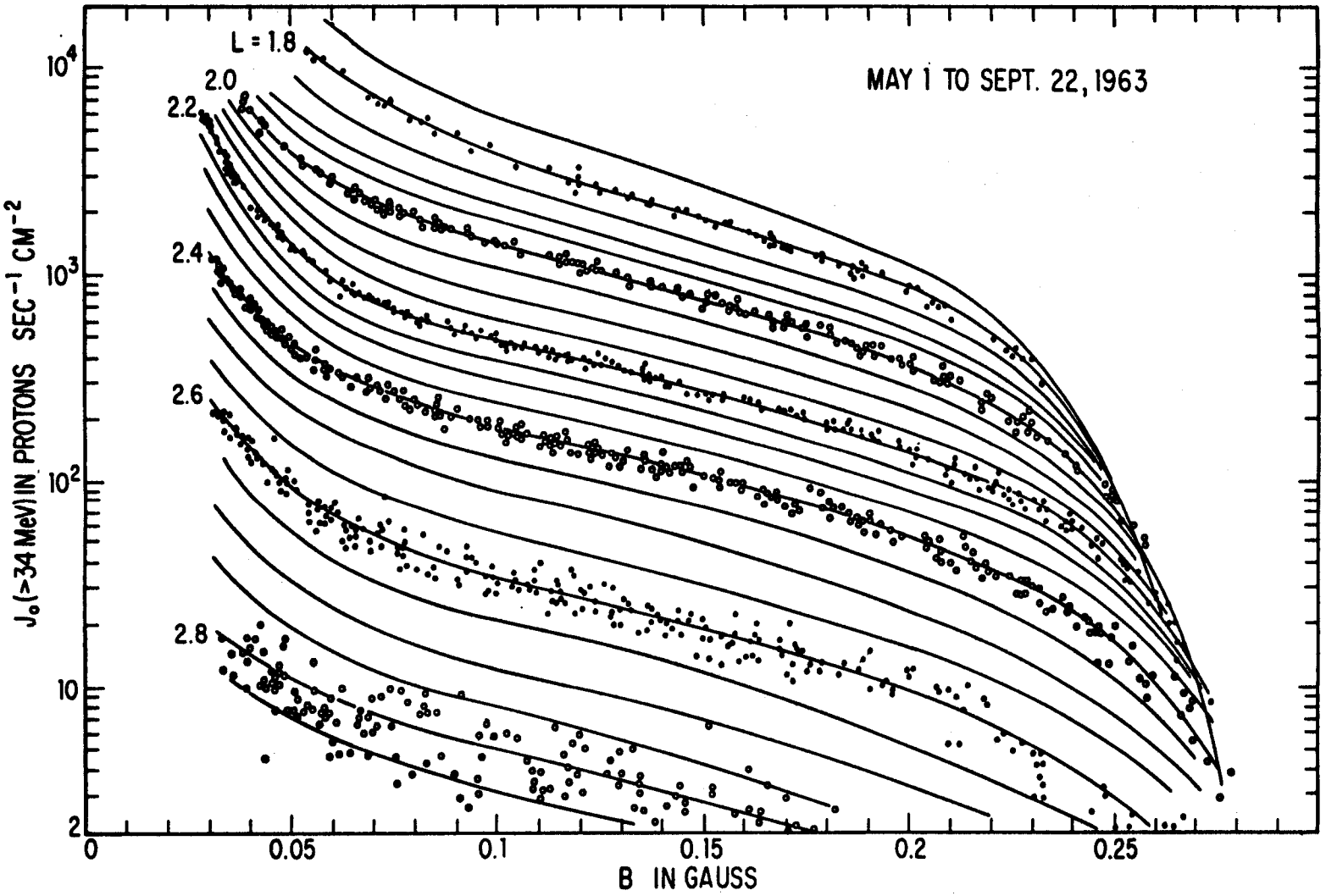
L = 1.8
2.0
2.2
2.4
2.6
2.8
MAY 1 TO SEPT. 22, 1963
J_o(>34 MeV) IN PROTONS SEC^{-1} CM^{-2}
10^4
10^3
10^2
10
2
0
0.05
0.1
0.15
0.2
0.25
B IN GAUSS

Figure 2

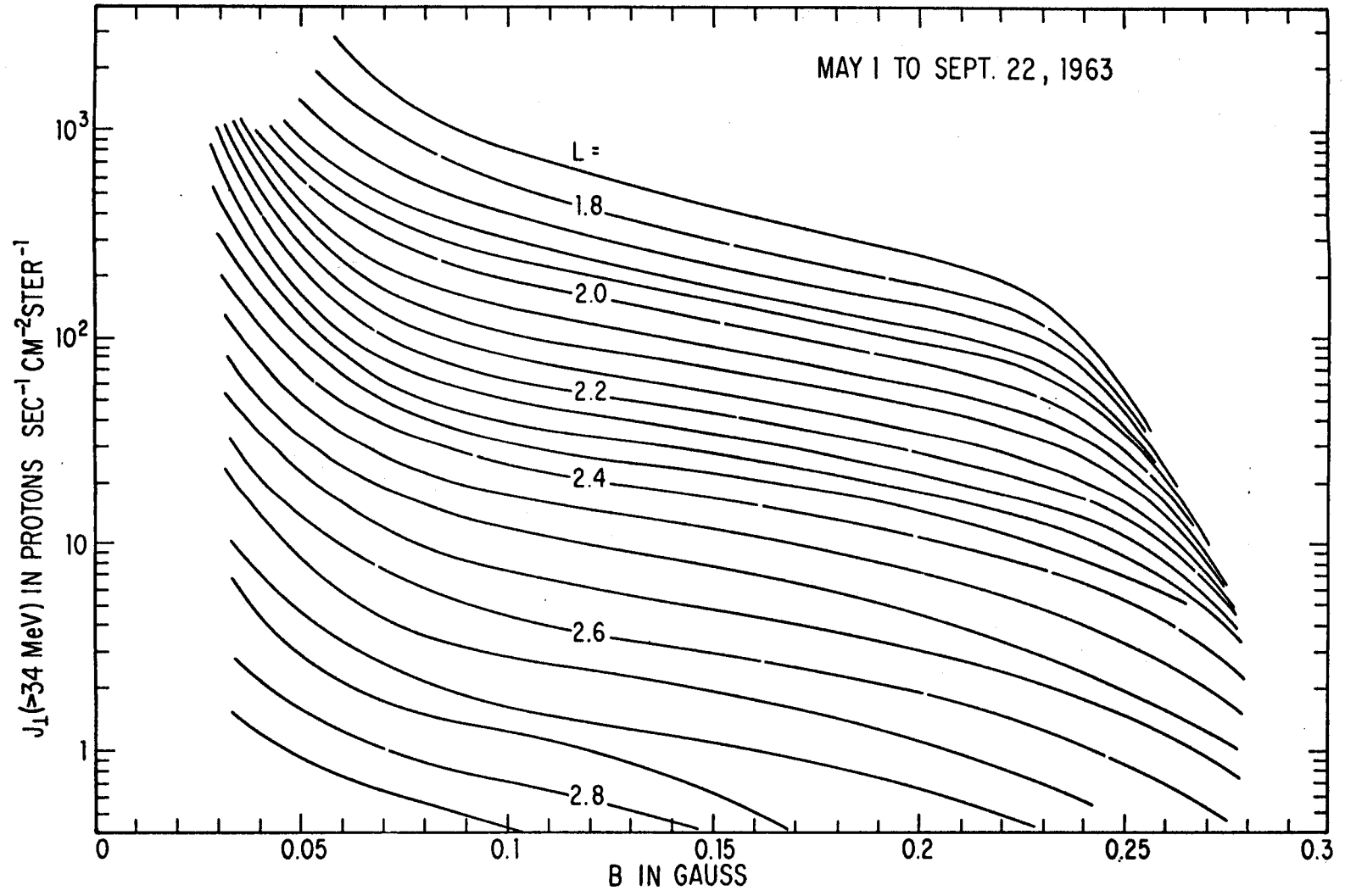
MAY 1 TO SEPT. 22, 1963
L =
1.8
2.0
2.2
2.4
2.6
2.8
10^3
10^2
10
1
$J_\perp$(>34 MeV) IN PROTONS SEC^{-1} CM^{-2}STER^{-1}
0
0.05
0.1
0.15
0.2
0.25
0.3
B IN GAUSS

Figure 3

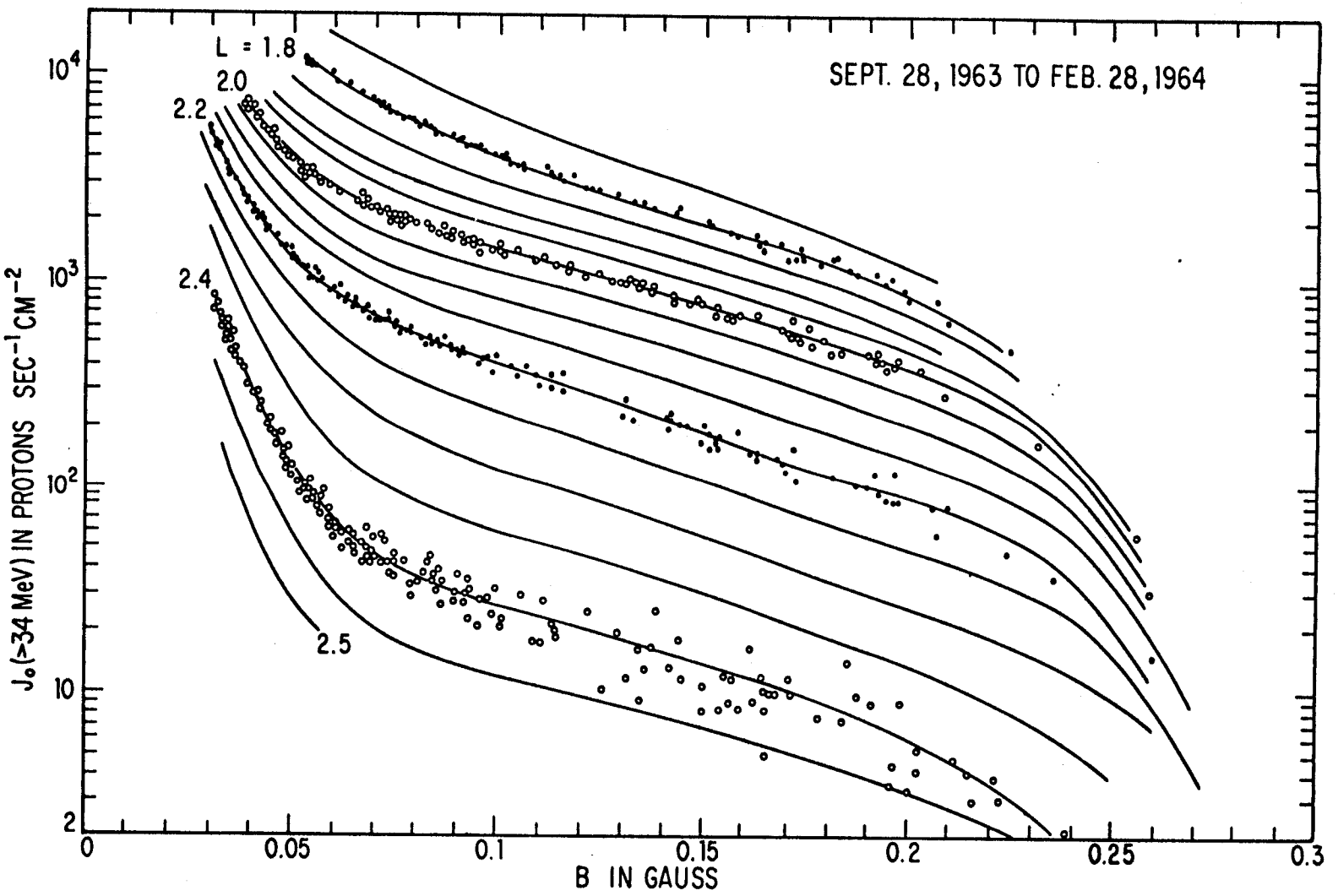
L = 1.8
2.0
2.2
2.4
2.5
SEPT. 28, 1963 TO FEB. 28, 1964
J_o(>34 MeV) IN PROTONS SEC^{-1}CM^{-2}
10^4
10^3
10^2
10
2
0
0.05
0.1
0.15
0.2
0.25
0.3
B IN GAUSS

Figure 4

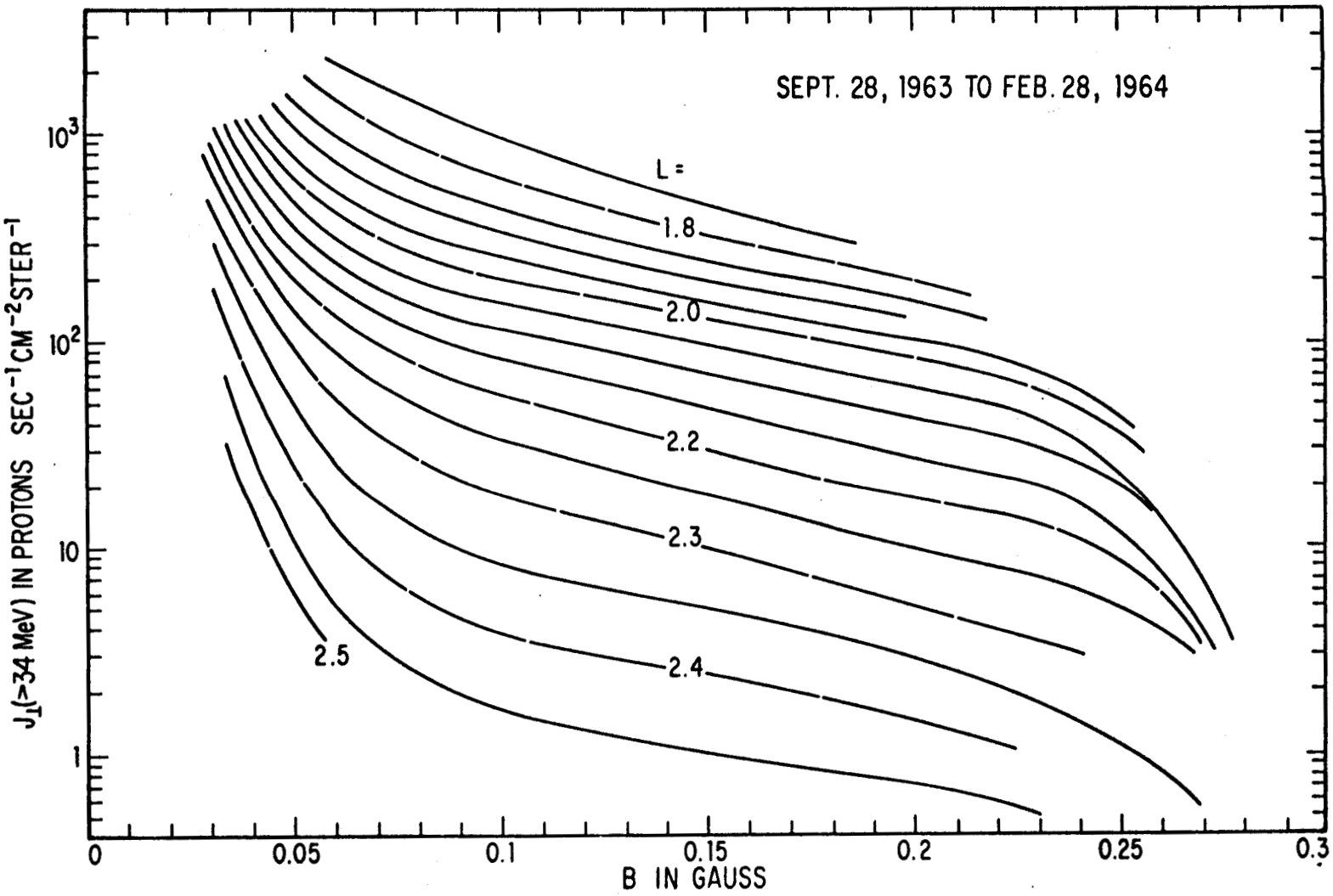
SEPT. 28, 1963 TO FEB. 28, 1964
L =
1.8
2.0
2.2
2.3
2.4
2.5
J_1(>34 MeV) IN PROTONS SEC^{-1}CM^{-2}STER^{-1}
10^3
10^2
10
1
0
0.05
0.1
0.15
0.2
0.25
0.3
B IN GAUSS

Figure 5

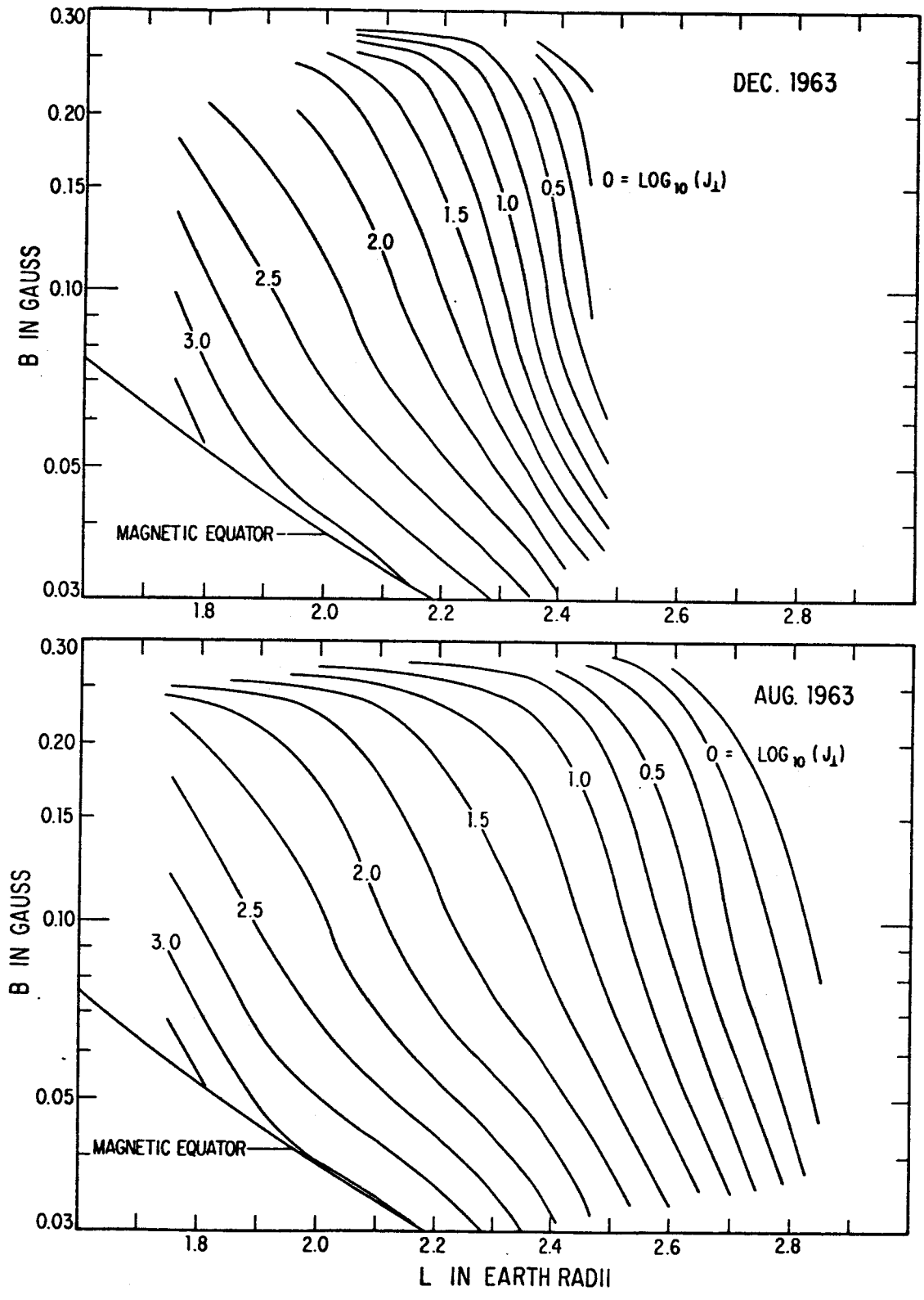
DEC. 1963
0 = LOG10 (J⊥)
0.5
1.0
1.5
2.0
2.5
3.0
MAGNETIC EQUATOR
B IN GAUSS
0.30
0.20
0.15
0.10
0.05
0.03
1.8
2.0
2.2
2.4
2.6
2.8
AUG. 1963
0 = LOG10 (J⊥)
0.5
1.0
1.5
2.0
2.5
3.0
MAGNETIC EQUATOR
B IN GAUSS
L IN EARTH RADII

Figure 6

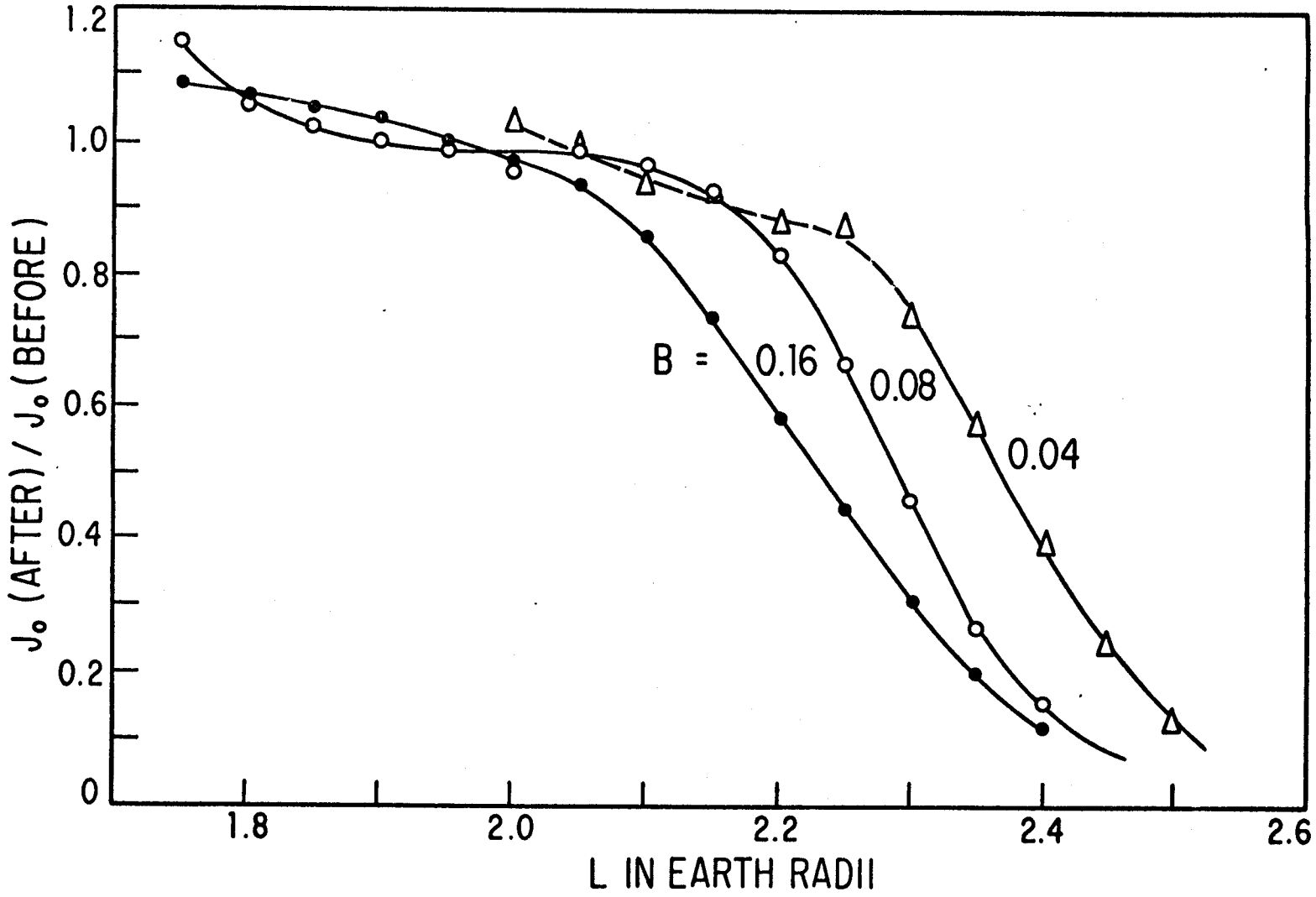
1.2
1.0
0.8
0.6
0.4
0.2
0
J_o (AFTER) / J_o (BEFORE)
B = 0.16
0.08
0.04
1.8
2.0
2.2
2.4
2.6
L IN EARTH RADII

Figure 7

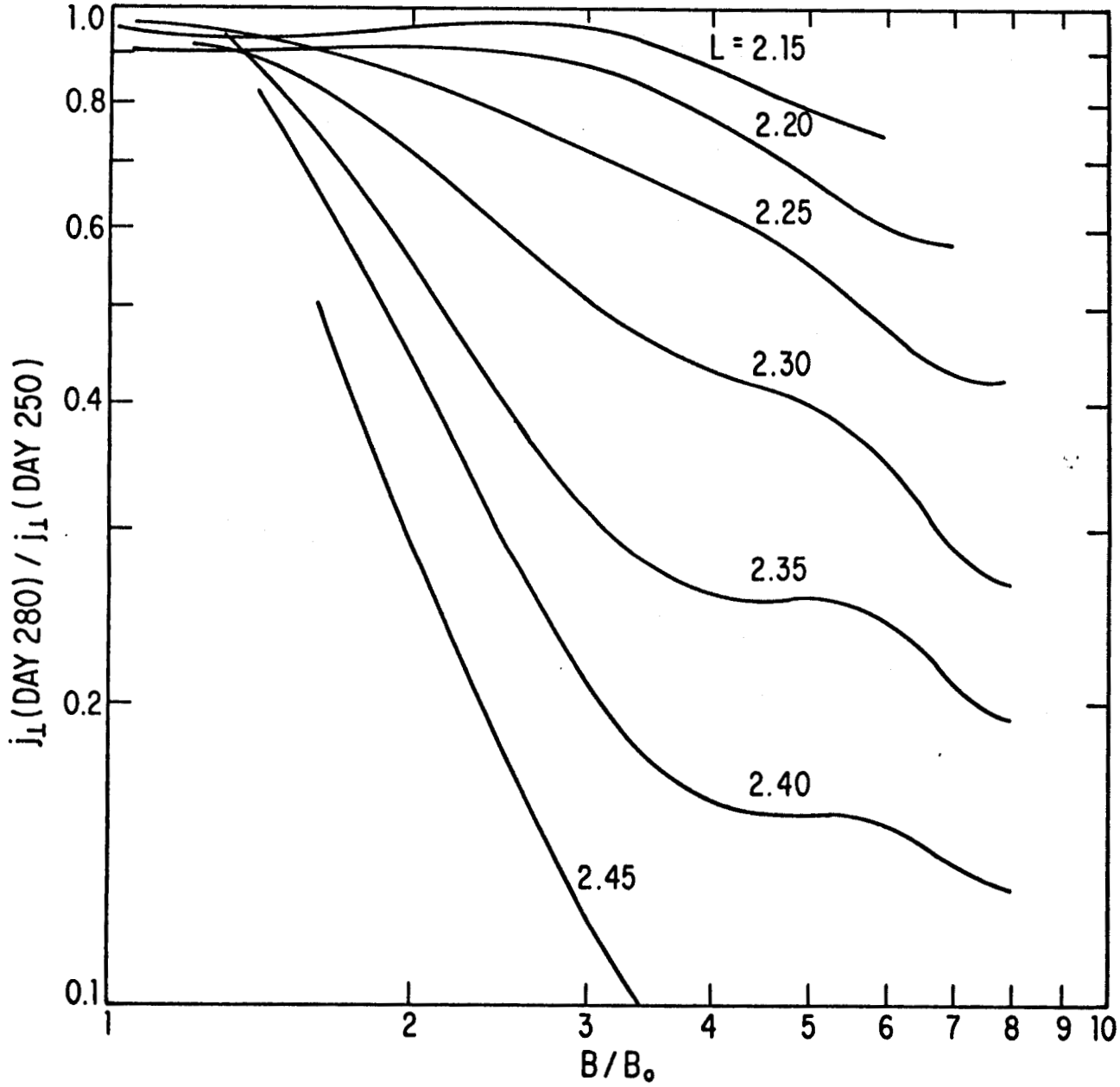
1.0
0.8
0.6
0.4
0.2
0.1
L = 2.15
2.20
2.25
2.30
2.35
2.40
2.45
1
2
3
4
5
6
7
8
9
10
B/B₀
j⊥(DAY 280) / j⊥(DAY 250)

Figure 8

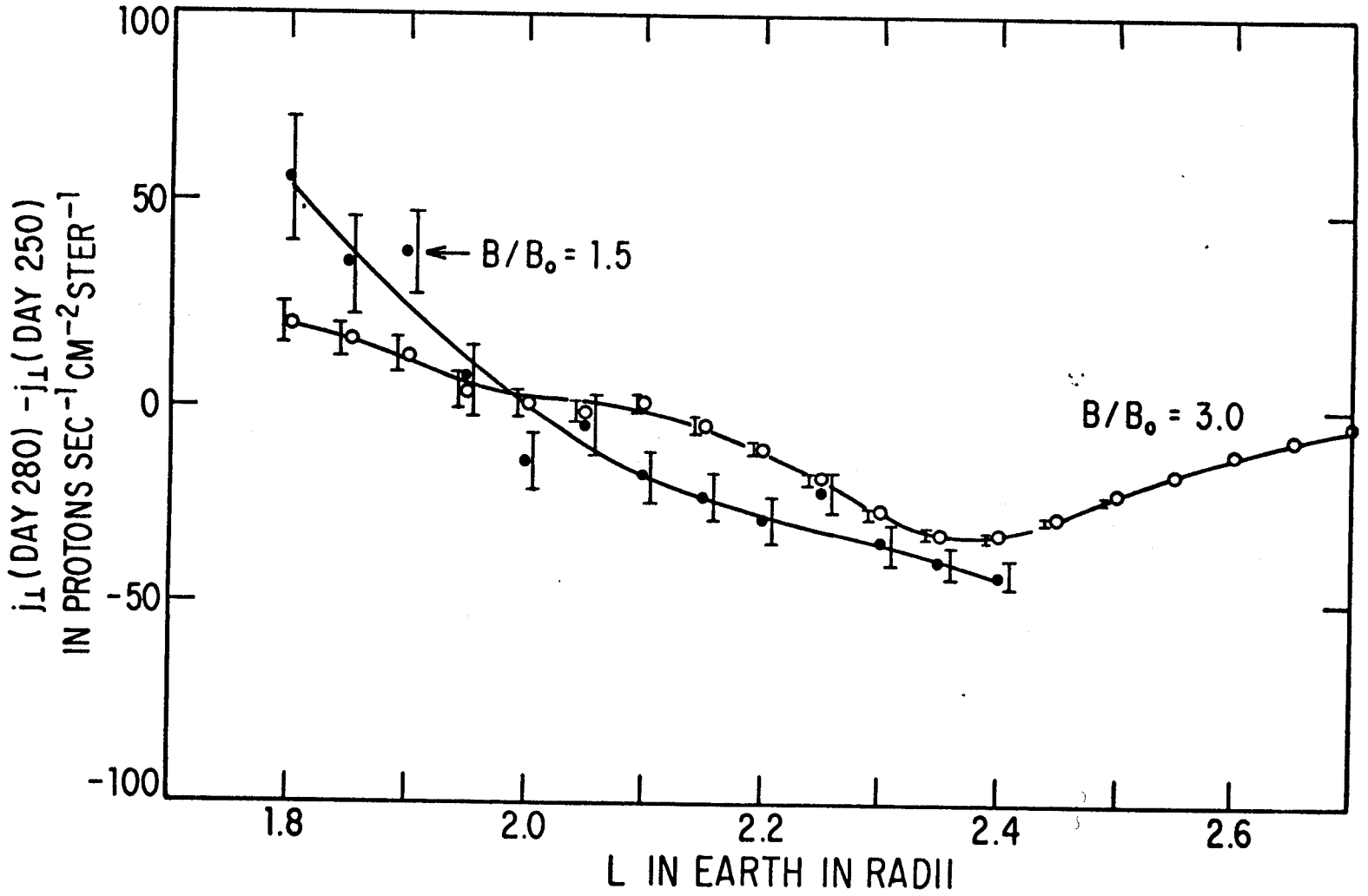
100
50
0
-50
-100
1.8
2.0
2.2
2.4
2.6
L IN EARTH IN RADII
$j_\perp$ (DAY 280) - $j_\perp$ (DAY 250)
IN PROTONS SEC^{-1}CM^{-2}STER^{-1}
B/B$_o$ = 1.5
B/B$_o$ = 3.0

Figure 9

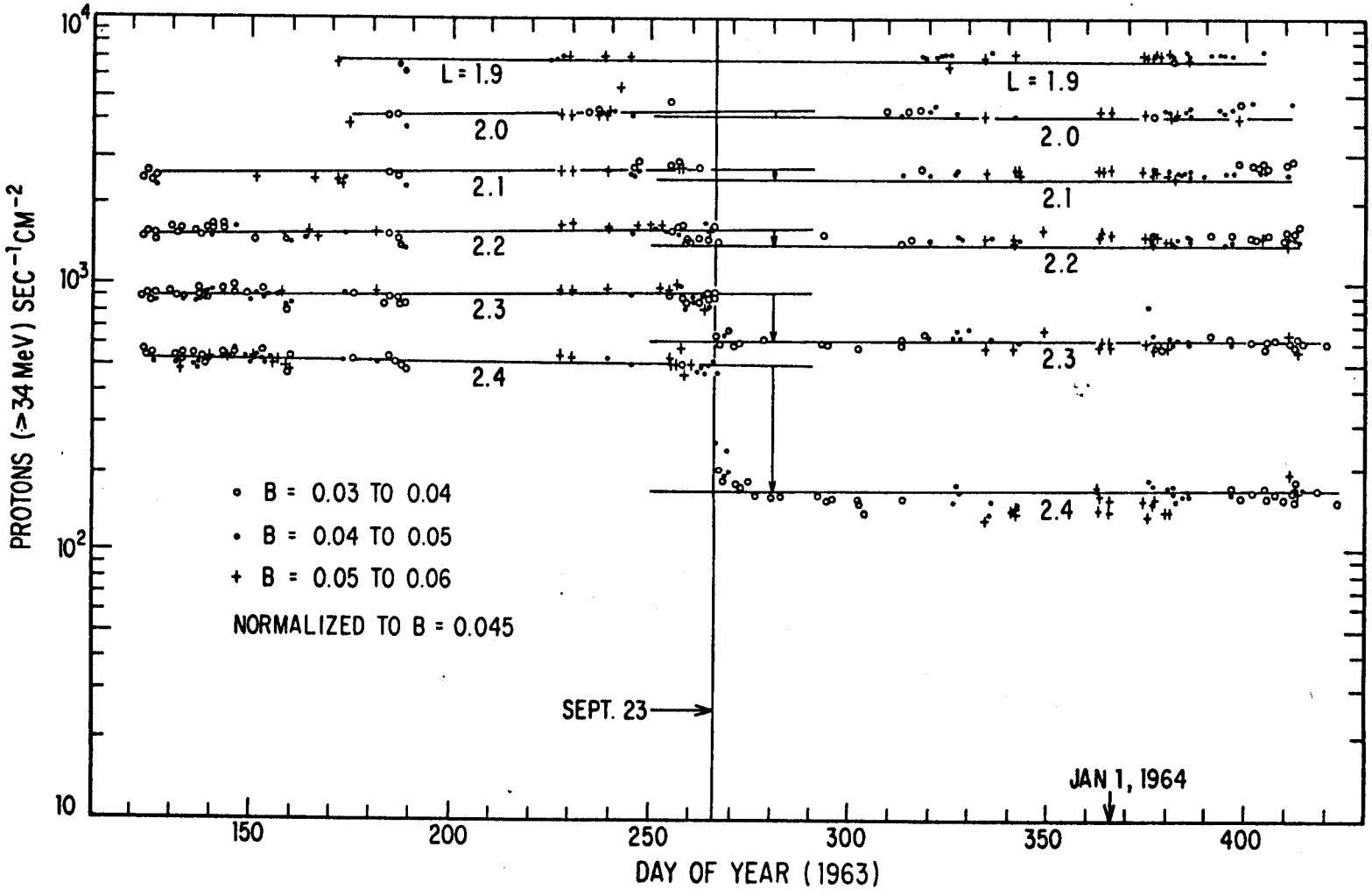
PROTONS (>34 MeV) SEC^{-1}CM^{-2}
10^4
10^3
10^2
10
L = 1.9
2.0
2.1
2.2
2.3
2.4
L = 1.9
2.0
2.1
2.2
2.3
2.4
○ B = 0.03 TO 0.04
• B = 0.04 TO 0.05
+ B = 0.05 TO 0.06
NORMALIZED TO B = 0.045
SEPT. 23
JAN 1, 1964
150
200
250
300
350
400
DAY OF YEAR (1963)

Figure 11

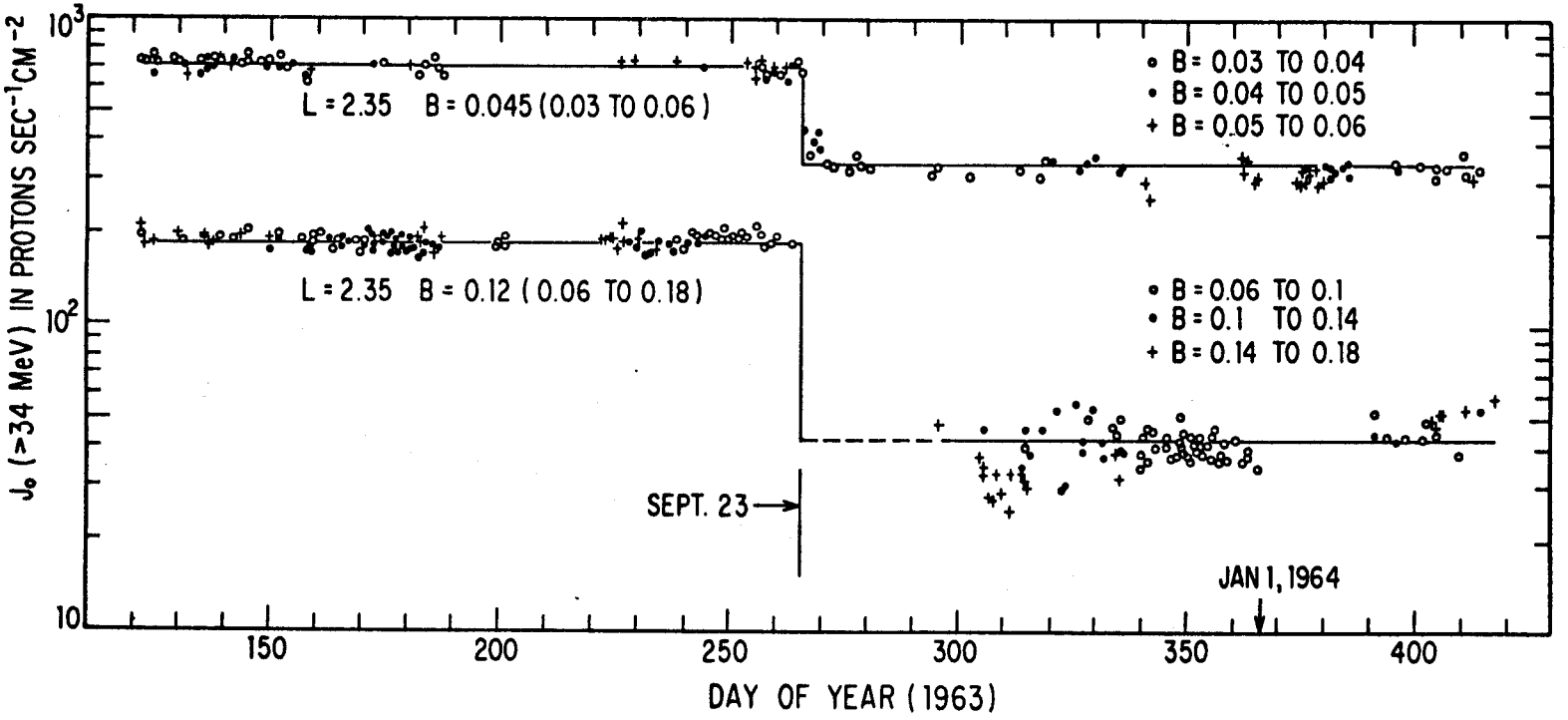
J_o (>34 MeV) IN PROTONS SEC^{-1}CM^{-2}
10^3
10^2
10
L = 2.35 B = 0.045 (0.03 TO 0.06)
L = 2.35 B = 0.12 (0.06 TO 0.18)
B = 0.03 TO 0.04
B = 0.04 TO 0.05
B = 0.05 TO 0.06
B = 0.06 TO 0.1
B = 0.1 TO 0.14
B = 0.14 TO 0.18
SEPT. 23
JAN 1, 1964
150
200
250
300
350
400
DAY OF YEAR (1963)

Figure 10

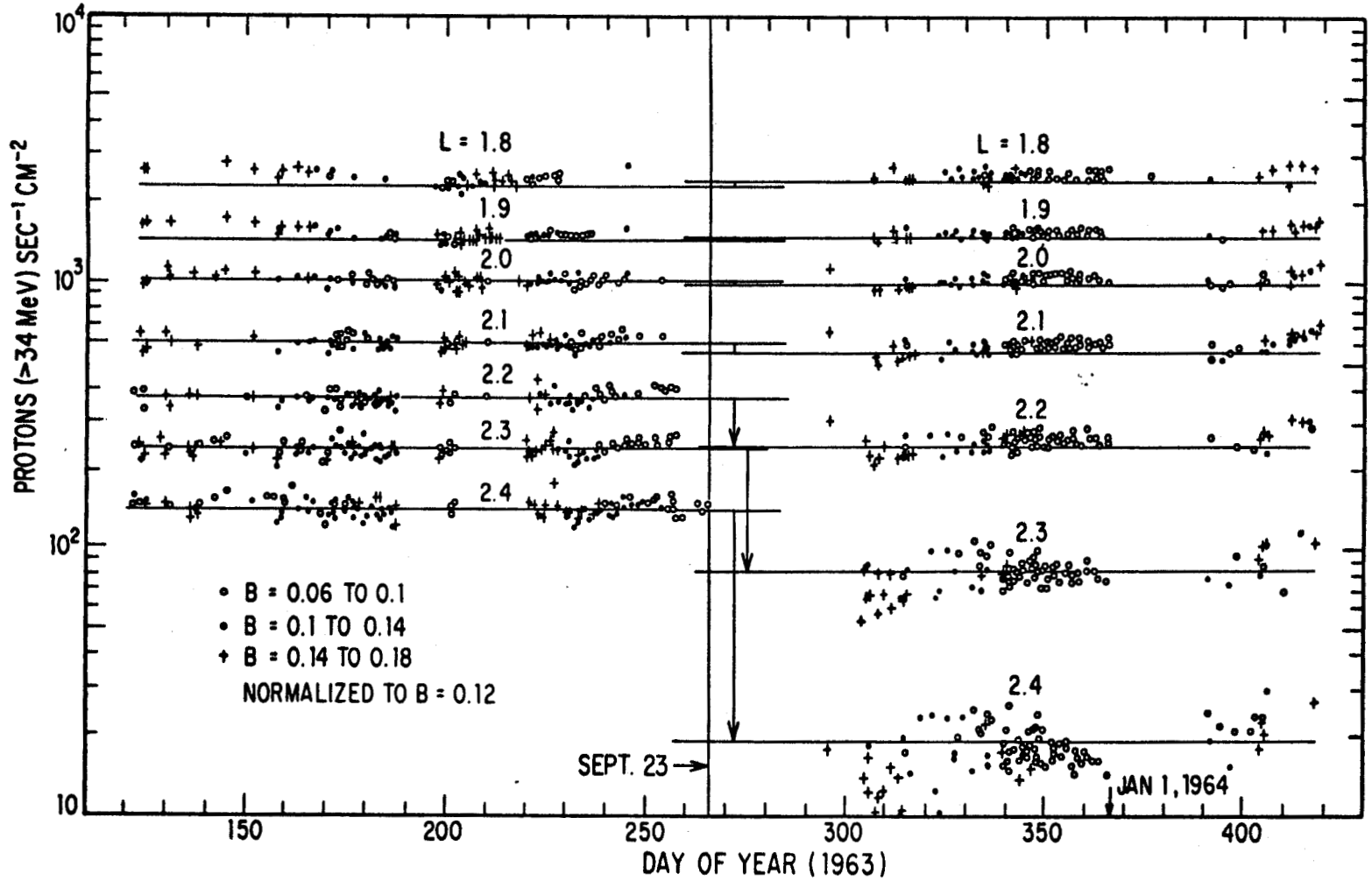
PROTONS (>34 MeV) SEC⁻¹ CM⁻²
10⁴
10³
10²
10
L = 1.8
1.9
2.0
2.1
2.2
2.3
2.4
• B = 0.06 TO 0.1
• B = 0.1 TO 0.14
+ B = 0.14 TO 0.18
NORMALIZED TO B = 0.12
SEPT. 23
JAN 1, 1964
150
200
250
300
350
400
DAY OF YEAR (1963)

Figure 12

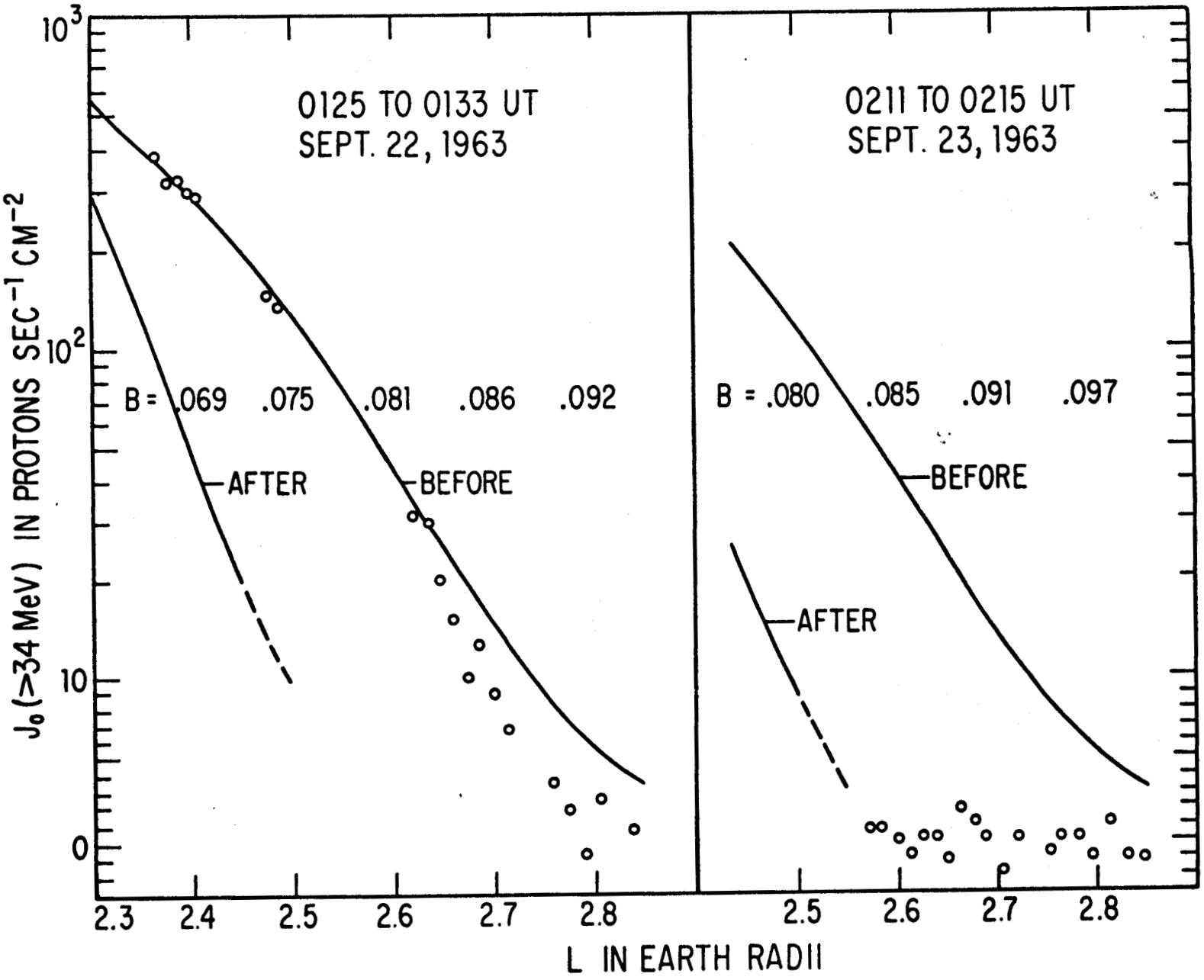
0125 TO 0133 UT
SEPT. 22, 1963
0211 TO 0215 UT
SEPT. 23, 1963
B = .069 .075 .081 .086 .092
B = .080 .085 .091 .097
AFTER
BEFORE
AFTER
BEFORE
J_0 (>34 MeV) IN PROTONS SEC^{-1} CM^{-2}
10^3
10^2
10
0
2.3 2.4 2.5 2.6 2.7 2.8
2.5 2.6 2.7 2.8
L IN EARTH RADII

Figure 13

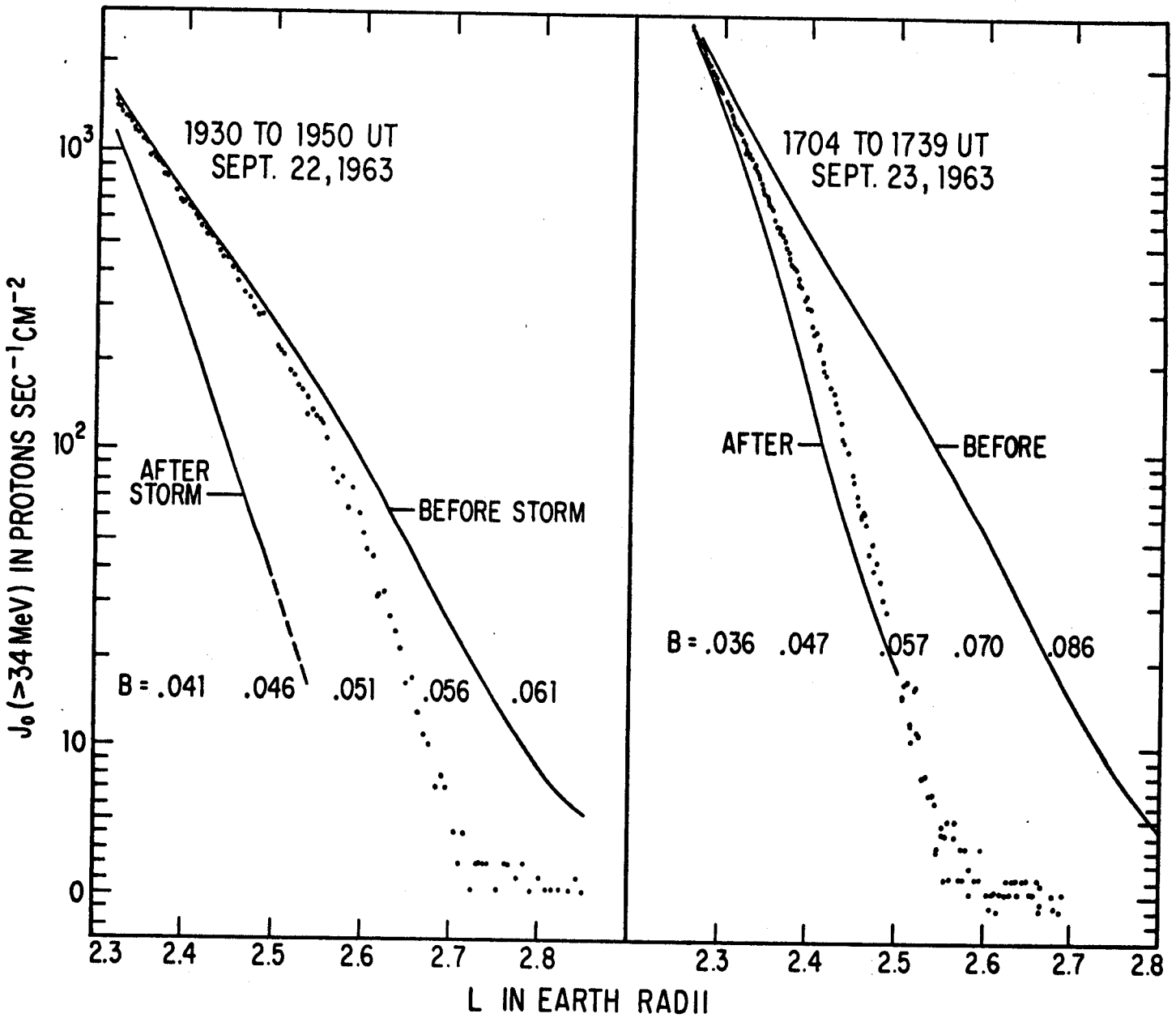
1930 TO 1950 UT
SEPT. 22, 1963
1704 TO 1739 UT
SEPT. 23, 1963
AFTER STORM
BEFORE STORM
AFTER
BEFORE
B = .041 .046 .051 .056 .061
B = .036 .047 .057 .070 .086
J_o (>34 MeV) IN PROTONS SEC^{-1}CM^{-2}
10^3
10^2
10
0
2.3 2.4 2.5 2.6 2.7 2.8
L IN EARTH RADII

Figure 14

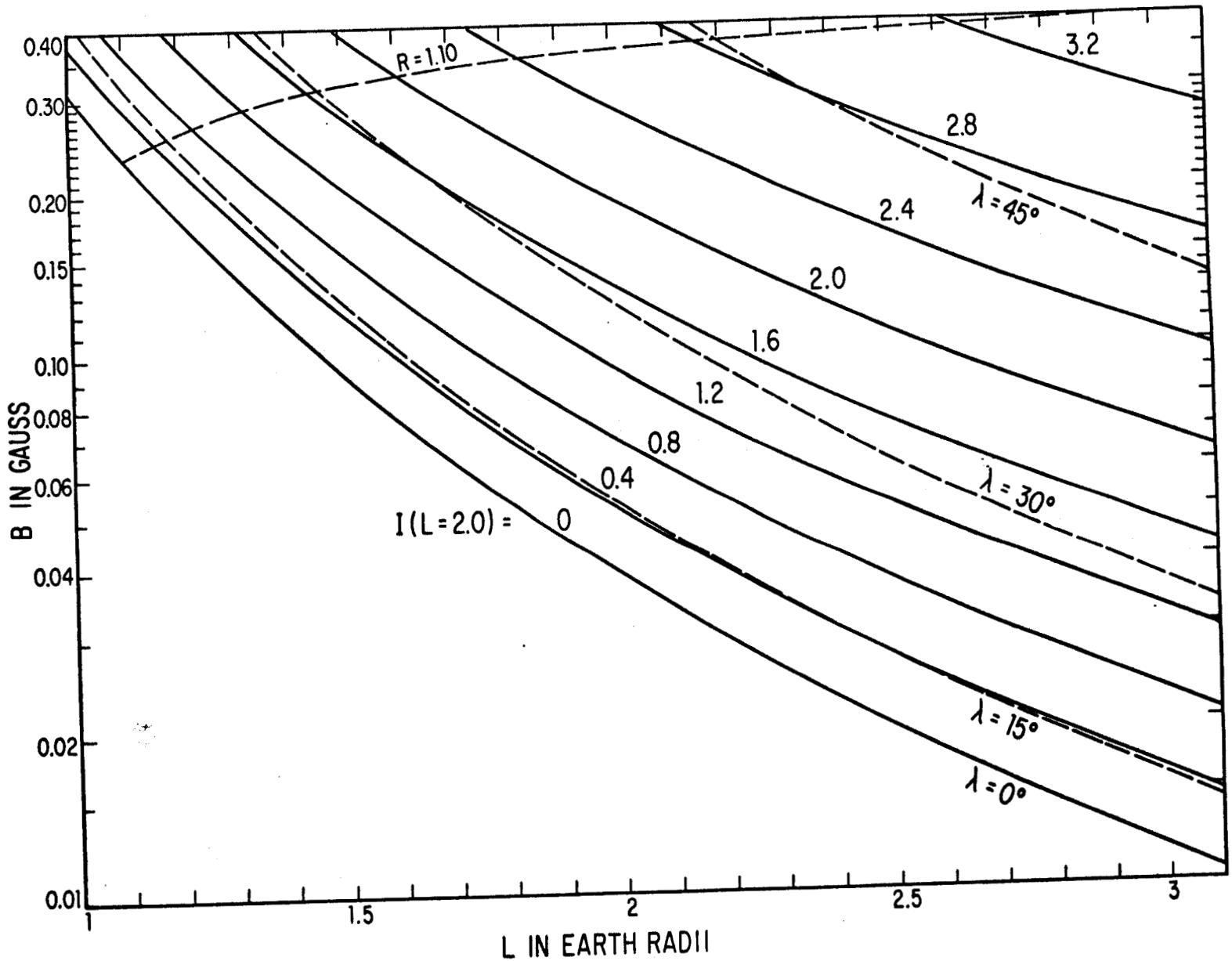
0.40
0.30
0.20
0.15
0.10
0.08
0.06
0.04
0.02
0.01
B IN GAUSS
R = 1.10
3.2
2.8
2.4
2.0
1.6
1.2
0.8
0.4
0
I (L = 2.0) =
λ = 45°
λ = 30°
λ = 15°
λ = 0°
1
1.5
2
2.5
3
L IN EARTH RADII

Figure 15